AD-A188 975 A MULTIPLE-ATTACK EFFECTIVENESS PREDICTION ALGORITHM 1/1
(U) SYNETICS CO DALLAS TEX J J PERRUZZI ET AL.
02 NOV 87 NUSC-TR-6652

UNCLASSIFIED F/G 15/6.2 NL

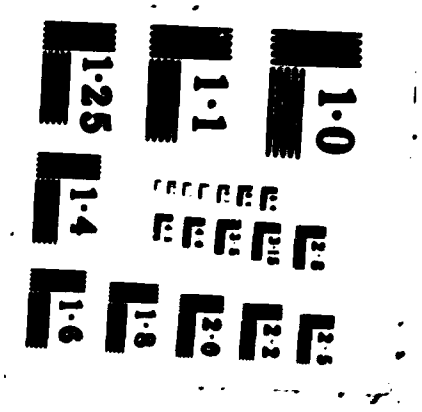
1.0
1.1
1.25
1.4
1.6

NUSC Technical Report 6682
2 November 1987

A Multiple-Attack Effectiveness Prediction Algorithm

J. J. Perruzzi
V. J. Aidala
Combat Control Systems Department

Naval Underwater Systems Center
Newport, Rhode Island / New London, Connecticut

REPORT DOCUMENTATION PAGE

1a. REPORT SECURITY CLASSIFICATION UNCLASSIFIED	1b. RESTRICTIVE MARKINGS
2a. SECURITY CLASSIFICATION AUTHORITY	3. DISTRIBUTION/AVAILABILITY OF REPORT Distribution authorized to U.S. Government agencies and their contractors only; administrative/operational use; 2 Nov 1987.
2b. DECLASSIFICATION/DOWNGRADING SCHEDULE	
4. PERFORMING ORGANIZATION REPORT NUMBER(S) TR 6652	5. MONITORING ORGANIZATION REPORT NUMBER(S)
6a. NAME OF PERFORMING ORGANIZATION Naval Underwater Systems Ctr 6b. OFFICE SYMBOL (If applicable) Code 2231	7a. NAME OF MONITORING ORGANIZATION
6c. ADDRESS (City, State, and ZIP Code) Newport Laboratory Newport, Rhode Island 02841	7b. ADDRESS (City, State, and ZIP Code)
8a. NAME OF FUNDING/SPONSORING ORGANIZATION Cheif of Naval Research 8b. OFFICE SYMBOL (If applicable) OCNR-232	9. PROCUREMENT INSTRUMENT IDENTIFICATION NUMBER
8c. ADDRESS (City, State, and ZIP Code) Washington, DC 20362	10. SOURCE OF FUNDING NUMBERS PROGRAM ELEMENT NO: PROJECT NO: RJ14F61 TASK NO: WORK UNIT ACCESSION NO:

11. TITLE (Include Security Classification)
A MULTIPLE-ATTACK EFFECTIVENESS PREDICTION ALGORITHM

12. PERSONAL AUTHOR(S)
Perruzzi, J.J., and Aidala, V.J.

13a. TYPE OF REPORT	13b. TIME COVERED	14. DATE OF REPORT (Year, Month, Day)	15. PAGE COUNT
Final	FROM ____ TO ____	87-11-02	29

16. SUPPLEMENTARY NOTATION

17. COSATI CODES			18. SUBJECT TERMS (Continue on reverse if necessary and identify by block number)
FIELD	GROUP	SUB-GROUP	Antisubmarine Warfare; Computational Algorithm; Multiple Attackers
15	01		
16	04		

19. ABSTRACT (Continue on reverse if necessary and identify by block number)

A model for predicting the effectiveness of multiple attackers against a single evader is analytically developed. Mathematical relationships are established that allow the probability of evader disablement or capture to be expressed in terms of attacker trajectory error statistics and destruction characteristics, as well as evader localization error statistics and evasion characteristics. These formulae are transformed into a compact computational algorithm, which allows attack effectiveness predictions to be made and updated on-line as a function of changing scenarios.

20. DISTRIBUTION/AVAILABILITY OF ABSTRACT	21. ABSTRACT SECURITY CLASSIFICATION
☐ UNCLASSIFIED/UNLIMITED ☒ SAME AS RPT ☐ DTIC USERS	UNCLASSIFIED

22a. NAME OF RESPONSIBLE INDIVIDUAL	22b. TELEPHONE (Include Area Code)	22c. OFFICE SYMBOL
J.J. Perruzzi	(401) 841-3703	Code 2231

DD FORM 1473, 84 MAR — 83 APR edition may be used until exhausted. All other editions are obsolete.

TABLE OF CONTENTS

LIST OF ILLUSTRATIONS

A MULTIPLE-ATTACK EFFECTIVENESS PREDICTION ALGORITHM

1. INTRODUCTION

When launching a multiple attack against an evader, there are several questions that must be considered. Among these are: When is the best time to launch? How many attackers should be deployed? What are the optimal attack trajectories? To begin to answer these questions, a real-time computational procedure is needed that predicts the effectiveness of multiple attackers against a prescribed invader.

One measure of attack effectiveness is given by the radial distance between evader and attacker at a specified termination time. Varying degrees of damage can be inflicted by simply placing the attacker in proximity to the evader at that time. Accordingly, range from attacker to evader is perhaps the single most important parameter affecting performance in any particular situation. Under realistic operating conditions, discrepancies between the actual and estimated values of range will invariably occur because of attacker delivery errors, as well as errors inherent in localizing the evader. To reliably predict attack performance, these errors must be accurately modeled.

Such a model is developed analytically in this report. The model allows the probability of evader disablement to be computed as a function of attacker characteristics, evader characteristics, and associated error statistics. The factors that significantly contribute to overall attack effectiveness are quantified. Typical inputs include (1) evader localization error statistics and the associated position and velocity estimates, (2) evader evasion characteristics, (3) attacker trajectory error statistics, (4) attacker destruction characteristics, (5) mean evader position after alertment, and (6) an offset between the mean evader position and attacker termination point. The model is subsequently transformed into a compact computational algorithm suitable for making online attack performance predictions.

In section 2, the problem is formulated and equations for the probability of evader disablement are developed. Section 3 provides simplifying approximations to the probability distributions, and section 4 presents a closed-form expression for the probability of evader disablement. In section 5, the results are modified to include multiple attacks launched against a single evader.

2. PROBLEM FORMULATION

Consider the geometric description of an attacker and evader encounter depicted in figure 1. Initially, the attacker is launched on a trajectory specified by the vector $\hat{\underline{X}}_w' = (\hat{X}_w\ \hat{Y}_w)$, where the prime symbol denotes matrix transposition. However, because of inherent errors in the delivery system, the attacker will not necessarily impact at its intended termination point. To accommodate possible discrepancies between these two points, the actual attacker position at time of termination is denoted by $\underline{X}_w' = (X_w, Y_w)$. For computational convenience, all errors associated with attacker positioning are tacitly assumed to be Gaussian-distributed with the following statistics:

$$E[\underline{X}_w] = \hat{\underline{X}}_w \ , \tag{1a}$$

$$E[(\underline{X}w - \hat{\underline{X}}_w)(\underline{X}_w - \hat{\underline{X}}_w)'] = P_w, \tag{1b}$$

where $E[\cdot]$ is the statistical expectation operator.

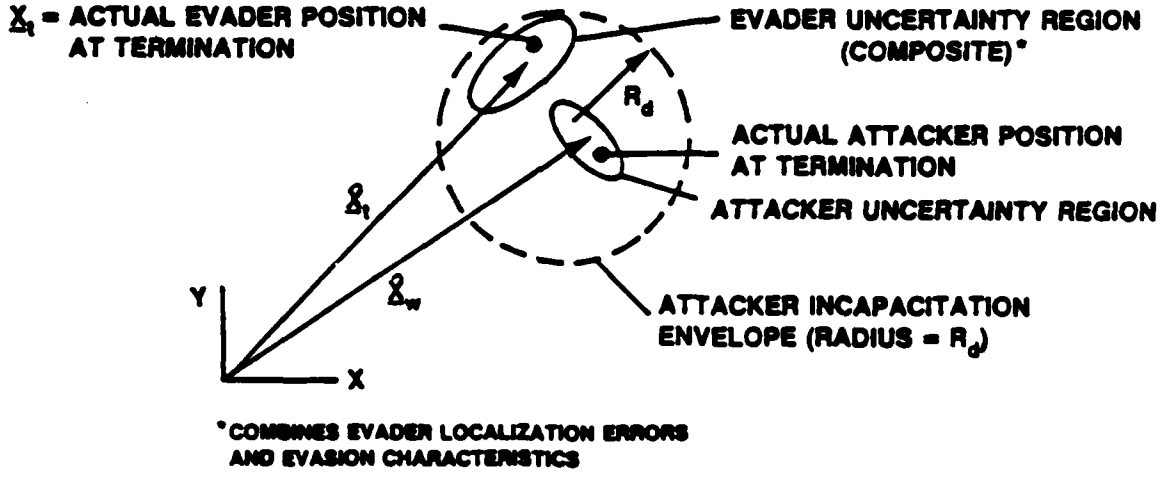

Figure 1. Geometric Description of Attacker/Evader Encounter

In a similar manner, the actual and estimated values of evader position at time of termination are defined by $\underline{X}_t' = (X_t, Y_t)$ and $\hat{\underline{X}}_t' = (\hat{X}_t, \hat{Y}_t)$, respectively. To determine the statistical characteristics of $\underline{X}_t$, observe that (see figure 2)

$$\underline{X}_t = \underline{X}_{to} + \underline{X}_{ta} \ , \tag{2}$$

where $\underline{X}_{to}$ represents evader position at alertment of an attack. Estimates of the vector $\underline{X}_{to}$ are typically obtained from localization and motion

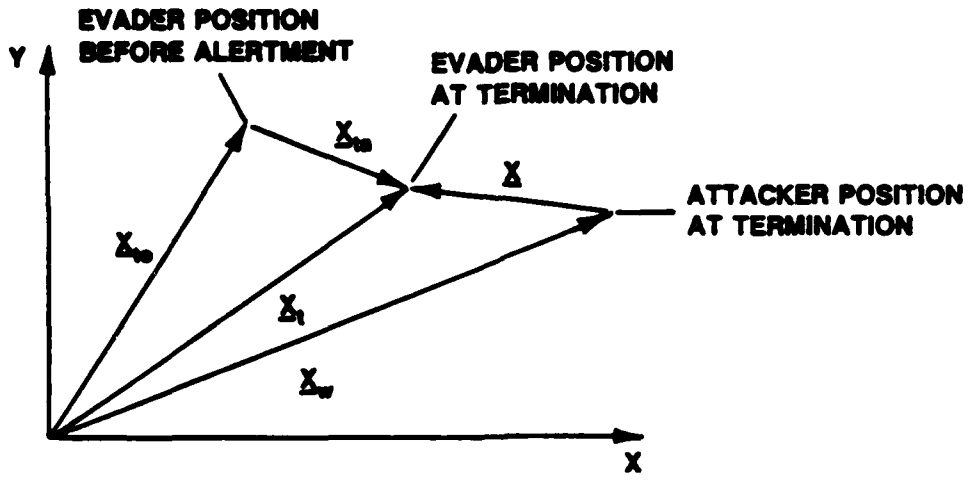

Figure 2. Vector Diagram of Relative Evader Position at Termination

analysis algorithms, which may also provide statistical descriptions of the associated estimation errors. Since these errors are modeled as Gaussian random variables (reference 1), $\underline{X}_{to}$ will also be Gaussian-distributed, with mean and covariance given by

$$E[\underline{X}_{to}] = \hat{\underline{X}}_{to} \ , \tag{3a}$$

$$E[(\underline{X}_{to} - \hat{\underline{X}}_{to})(X_{to} - \hat{\underline{X}}_{to})'] = P_{to} \ . \tag{3b}$$

The vector $\underline{X}_{ta}$ defines the evader position at time of termination relative to its position at time of alertment. Unfortunately, errors associated with estimating $\underline{X}_{ta}$ have a complicated non-Gaussian probability distribution that functionally depends on the evasion characteristics. To devise tractable approximations for this distribution requires a suitable geometric model of the evader escape region. The simplest model is a circle centered at $\underline{X}_{to}$ whose radius increases with time in proportion to the maximum evader speed. Although such models are frequently used in practical applications, they are somewhat unrealistic because they implicitly assume that the evader has a zero turning radius. Recently, more realistic techniques of modeling evader evasion characteristics have been developed (reference 2). The resulting escape regions, shown in figure 3, accurately reflect constraints on the evader dynamics by utilizing a non-zero turning radius in conjunction with a finite maximum speed. At any prescribed time

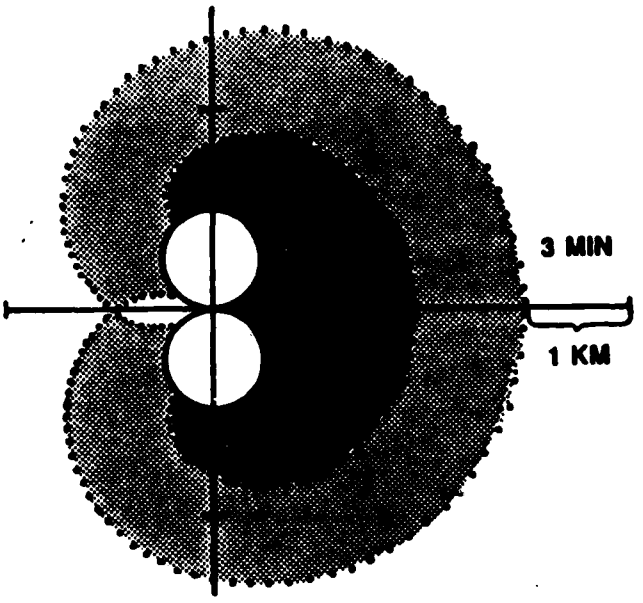

Figure 3. Growth of Evader Escape Region with Time

after alertment, the evader must reside within a region whose boundary consists of an involute (dotted curve in figure 3) and arcs of the two minimum-turning-radius circles.

As an example, the darkest shaded area in figure 3 depicts the evader escape region at 1 minute after alertment. In this illustration, the origin of coordinates is defined by the vector $\underline{X}_{to}$ (the assumed evader position at alertment).

Because the actual escape region is difficult to describe analytically, it will be approximated by a circumscribing circle as shown in figure 4. Although this approximation introduces errors into subsequent probability computations, these errors decrease with time because the actual and approximate escape regions eventually coincide (reference 2). For convenience of notation, R_e is used to denote the radius of the circumscribing circle, and $\hat{\underline{X}}_{ta}$ defines the location of its center relative to $\underline{X}_{to}$.

While it is known that an alerted evader must necessarily reside within a prescribed escape region, more specific data to further refine the localization process are usually unavailable. Evasive maneuvers are almost certain to occur because of the crisis nature of the situation (i.e., the evader knows it is under attack). However, the absence of additional information precludes classifying, in general, one type of maneuver as more likely than another. In light of this fact, it is not unreasonable to assume that the errors associated with estimating $\underline{X}_{ta}$ are uniformly distributed over the prescribed escape region. Under such an assumption, it can be shown that

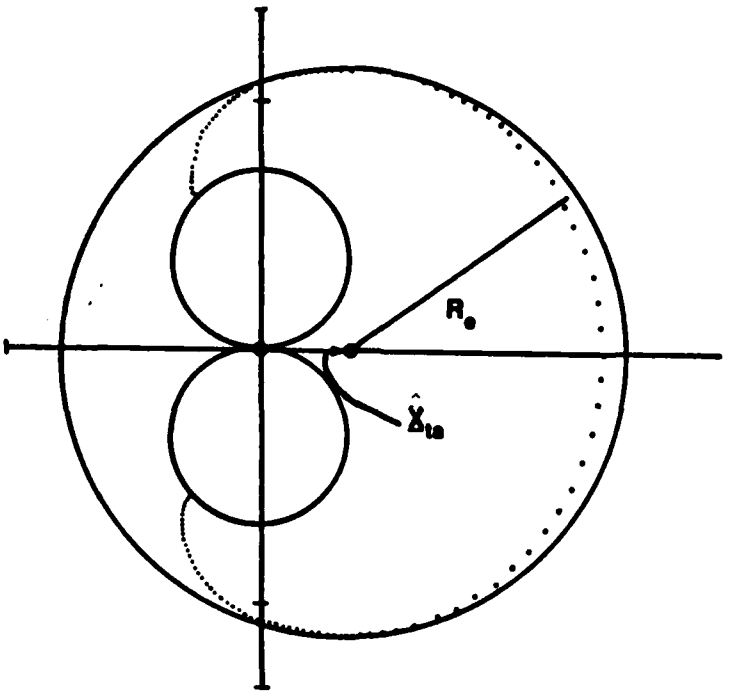

Figure 4. Circular Approximation of Evader Escape Region

$$E[\underline{X}_{ta}] = \hat{\underline{X}}_{ta} \ , \tag{4a}$$

$$E[(\underline{X}_{ta} - \hat{\underline{X}}_{ta})(\underline{X}_{ta} - \hat{\underline{X}}_{ta})'] = (R_e/2)^2 \ I \ , \tag{4b}$$

where I is the two-dimensional identity matrix, and the pertinent statistical computations are performed using a circular approximation as depicted in figure 4.

To determine the probability of evader disablement resulting from an attack, it is necessary to mathematically combine the statistical information embodied in equations (1) through (4) with known attacker damage characteristics. This task may be accomplished via application of the law of total probability (reference 3), which leads to the expression

$$\text{Prob}[EI] = \int_{\Omega} \text{Prob}[EI|R]p(R)dR, \tag{5}$$

where $R = |\underline{X}|$ is the range from evader to attacker at time of termination, and Ω is the set of all possible values of R. Here, the conditional probability function, Prob[EI|R], defines the probability of evader disablement given that the relative range from attacker to evader is known at time of termination. It is this term that incorporates attacker destruction characteristics into the effectiveness prediction model. The remaining term p(R) represents the probability density of R and is used to account for evader localization errors and evasion characteristics, as well as attacker

trajectory errors. To see this, observe from figure 2 that the vector $\underline{X}$ can be written as

$$\underline{X} = \underline{X}_{to} + \underline{X}_{ta} - \underline{X}_{w} \cdot \tag{6}$$

Thus, both the magnitude and direction of $\underline{X}$ is affected by evader localization errors via $\underline{X}_{to}$, evasion characteristics via $\underline{X}_{ta}$, and trajectory errors via $\underline{X}_{w}$.

To compute the probability of disablement online and in real time, it is first necessary to explicitly represent p(R) and Prob[EI|R] as integrable functions of R. Unfortunately, it is virtually impossible to develop exact mathematical representations of these two functions that are amenable to closed-form integration. Nevertheless, suitable approximations can be employed, allowing equation (5) to be evaluated without recourse to numerical integration. The desired approximations for p(R) and Prob[EI|R] are computed in the next section.

3. APPROXIMATION OF THE PROBABILITY DISTRIBUTION

To mathematically describe the probability density, p(R), it is convenient to utilize the concept of characteristic functions (reference 3). For the problem under consideration, observe from equation (6) that the vector $\underline{X}$ is a linear function $\underline{X}_{to}$, $\underline{X}_{ta}$, and $\underline{X}_w$. Since the errors associated with estimating these latter three vectors are uncorrelated, it follows (reference 3) that the characteristic function of $p(\underline{X})$ satifies the relation

$$\Phi_X(\underline{\omega}) = \Phi_{to}(\underline{\omega})\Phi_{ta}(\underline{\omega})\Phi_w(-\underline{\omega}) \ , \tag{7}$$

where $\Phi_{to}(\underline{\omega})$, $\Phi_{ta}(\underline{\omega})$, and $\Phi_w(\underline{\omega})$ are characteristic functions of the probability densities $p(\underline{X}_{to})$, $p(\underline{X}_{ta})$, and $p(\underline{X}_w)$, respectively. In view of the assumption that $\underline{X}_{to}$ and $\underline{X}_w$ are Gaussian-distributed, the functions $\Phi_{to}(\underline{\omega})$ and $\Phi_w(\underline{\omega})$ take the form (reference 3)

$$\Phi_{to}(\underline{\omega}) = \exp[j\underline{\omega}'\hat{\underline{X}}_{to} - (1/2)\underline{\omega}'P_{to}\underline{\omega}] \ , \tag{8}$$

$$\Phi_w(\underline{\omega}) = \exp(j\underline{\omega}'\hat{\underline{X}}_w - (1/2)\underline{\omega}'P_w\underline{\omega}] \ . \tag{9}$$

As discussed previously, the vector $\underline{X}_{ta}$ is presumed to be uniformly distributed over the evader region; thus

$$p(\underline{X}_{ta}) = \begin{cases} \dfrac{1}{\pi Re^2} & |\underline{X}_{ta} - \hat{\underline{X}}_{ta}| \leq Re \\ 0 & |\underline{X}_{ta} - \hat{\underline{X}}_{ta}| > Re \end{cases} . \tag{10}$$

Although this expression may be utilized without alteration, it will facilitate subsequent computations to approximate $p(\underline{X}_{ta})$ via the formula

$$p(\underline{X}_{ta}) \quad p_n(\underline{X}_{ta}) = \left[\frac{n+1}{n}\right]\left[\frac{\exp[-(n+1)p^2]}{\pi R_e^2}\right]\sum_{k=0}^{n-1}\frac{(n+1)^k}{k!}p^{2k} \ . \tag{11}$$

Here, n determines the order of the approximating series, and

$$p = \frac{|\underline{X}_{ta} - \hat{\underline{X}}_{ta}|}{R_e} \ . \tag{12}$$

The finite-sum Gaussian distributions described in equation (11) are often used to evaluate complicated probability integrals in terms of elementary functions.

The characteristic function for $p_n(\underline{X}_{ta})$ is given by

$$\Phi_{ta}(\underline{\omega};n) = \frac{1}{n}L_{n-1}^{(1)}\left[\frac{1}{2}p_e\omega^2\right]\exp[j\omega'\underline{X}_{ta} - \frac{1}{2}p_e\omega^2] \ , \tag{13}$$

where

$$\omega = ||\underline{\omega}|| = \sqrt{\omega_x^2 + \omega_y^2} \ , \tag{14}$$

$$p_e = \frac{R_e^2}{2(n+1)} \ , \tag{15}$$

and $L_m^{(p)}[\cdot]$ are Laguerre polynomials (reference 4) defined by

$$L_m^{(p)}[\xi] = \sum_{k=0}^{m} \binom{m+p}{m-k} \frac{1}{k!} (-\xi)^k \quad m,p = 0,1,2,\ldots \ . \tag{16}$$

Here, n appears as an argument in the characteristic function of $p_n(\underline{X}_{ta})$ to denote the order of the approximating series.

Since equations (7), (8), (9), and (13) completely specify the characteristic function of $p(\underline{X})$, this probability density may be determined analytically as follows:

$$p(\underline{X}) = \frac{1}{(2\pi)^2} \int_{-\infty}^{\infty}\int_{-\infty}^{\infty} \Phi_X(\underline{\omega}) \exp[-j\underline{\omega}'\underline{X}]d\underline{\omega} \ . \tag{17}$$

To obtain the distribution of range errors, a transformation to polar coordinates is made, such that

$$p(R,\theta) = p(\underline{X})||J|| = \frac{R}{(2\pi)^2} \int_{-\infty}^{\infty}\int_{-\infty}^{\infty} \Phi_X(\underline{\omega}) \exp[-j\underline{\omega}R \cos(\theta - \Phi)]d\underline{\omega} \ , \tag{18}$$

where

$$\Phi = \tan^{-1}(\omega_y/\omega_x) \ . \tag{19}$$

The desired probability density $p(R)$ follows by integrating $p(R,\theta)$ over the interval $0 \leq \theta \leq 2\pi$; that is,

$$\begin{aligned} p(R) &= \int_0^{2\pi} p(R,\theta)d\theta \\ &= \frac{R}{(2\pi)^2} \int_{-\infty}^{\infty}\int_{-\infty}^{\infty} \Phi_X(\underline{\omega}) \left[\int_0^{2\pi} \exp[-j\underline{\omega}R \cos(\theta - \Phi)]\right] d\underline{\omega} \\ &= \frac{1}{2\pi} \int_{-\infty}^{\infty}\int_{-\infty}^{\infty} \Phi_X(\underline{\omega}) R\, J_0(\underline{\omega}R)d\underline{\omega} \ , \end{aligned} \tag{20}$$

where $J_0(\omega R)$ is a zeroth order Bessel function (reference 5).

To mathematically describe the function Prob[EI|R] requires explicit knowledge of the attacker destruction characteristics. For this study, attackers with circular interdiction zones are used.

The center of the zone coincides with attacker position at time of termination. For computational convenience, R_d will be used to define the radius of the destruction envelope.

Although specific numerical data are available, an exact mathematical description of $P[EI|R]$ does not exist. However, from practical considerations, it is apparent that this function will decrease monotonically as R increases and also must satisfy the inequality

$$0 \leq P[EI|R] \leq 1 , \tag{21}$$

for $0 \leq R < \infty$. These characteristics suggest that finite-sum Gaussian distributions again be used as a basis for approximating $P[EI|R]$, i.e.,

$$P[EI|R] \approx P[EI|R,m] \tag{22}$$

where

$$P[EI|R,m] = \exp[-m\xi^2] \sum_{k=0}^{m-1} \frac{m^k}{k!} \xi^{2k} . \tag{23}$$

As before, m determines the order of the approximating series, and

$$\xi = R/R_d . \tag{24}$$

Graphs of equation (23) for $m = 1,2,3,\ldots, 10$ and $m = \infty$ are plotted in figure 5. As expected, these functions all decrease monotonically as R increases. Note also that the limiting conditional probability may be expressed in the form

$$P[EI|R,\infty] = \begin{cases} 1 & 0 \leq R \leq R_d \\ 0 & R > R_d \end{cases} . \tag{25}$$

Because of its simplicity, equation (25) is frequently used in practical applications even though it is somewhat artificial. Indeed, such an approximation implicitly assumed that attacks will have uniformly devastating effects over the entire attacker destruction envelope. In light of this, it is perhaps more realistic, and certainly more economical, to employ lower-order approximations when possible. Accordingly, the parameter m will not be specified here so as to enhance modeling flexibility and realism.

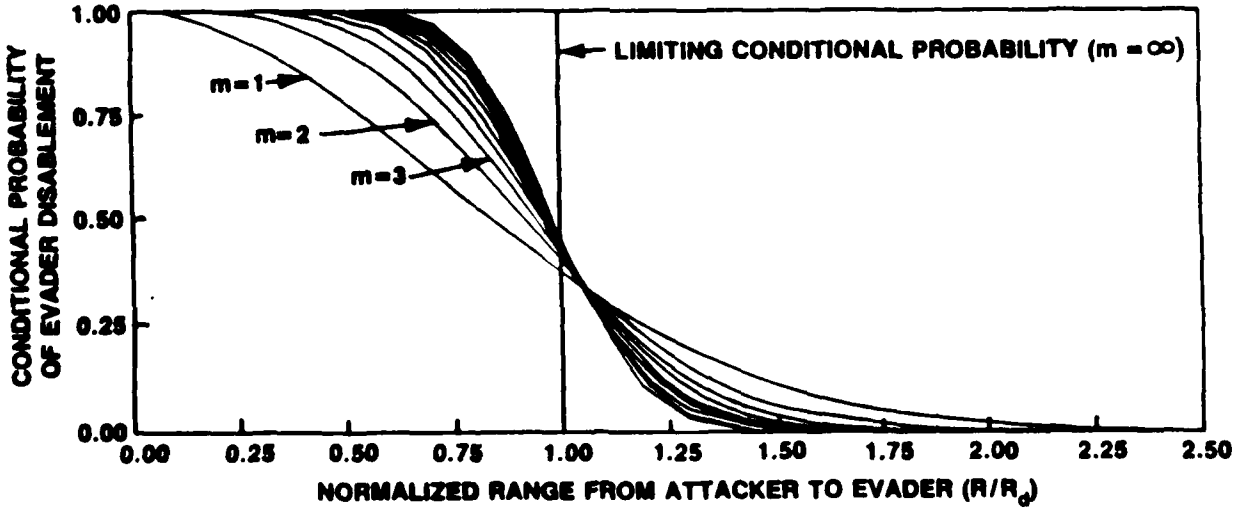

Figure 5. Plots of the Function $P[EI|R,m]$

Reverse Blank

4. COMPUTATION OF THE EVADER DISABLEMENT PROBABILITY

The probability of evader disablement resulting from an attack may now be determined analytically by utilizing approximations developed in section 3 in conjunction with the law of total probability. More precisely, substituting equations (20), (22), (23), and (24) into equation (5), and evaluating the resultant integral over Ω, leads to the expression

$$P[EI] = \int_{-\infty}^{\infty}\int_{-\infty}^{\infty} \Phi_X(\underline{\omega})\Psi(\underline{\omega})d\underline{\omega} \quad , \tag{26}$$

where

$$\Psi(\omega) = \frac{p_d}{2\pi} L_{m-1}^{(1)}\left[\frac{1}{2}p_d\omega^2\right] \exp[\tfrac{1}{2}p_d\omega^2] \quad , \tag{27}$$

$$p_d = R_d/2m \quad , \tag{28}$$

and $L_{m-1}^{(1)}[\bullet]$ is the Laguerre polynomial defined previously. In deriving equation (26), it might be noted that integration of the exact probability distributions over Ω is mathematically equivalent to integrating the approximate distributions over a semi-infinite interval $0 < R < \infty$.

If equations (7), (8), (9), (13), and (27) are combined, the integrand in equation (26) may be rewritten as

$$\Phi_X(\underline{\omega})\Psi(\underline{\omega}) = \frac{p_d}{2\pi n} L_{n-1}^{(1)}\left[\frac{1}{2}p_e\underline{\omega}^2\right] L_{m-1}^{(1)}\left[\frac{1}{2}p_d\underline{\omega}^2\right] \exp[j\underline{\omega}'\hat{\underline{X}} - \tfrac{1}{2}\omega' P\omega] \quad , \tag{29}$$

where

$$\hat{\underline{X}} = \begin{bmatrix}\hat{X}\\ \hat{Y}\end{bmatrix} = \hat{\underline{X}}_{to} + \hat{\underline{X}}_{ta} - \hat{\underline{X}}_{w} \quad , \tag{30}$$

$$P = \begin{bmatrix}P(1,1) & P(1,2)\\ P(1,2) & P(2,2)\end{bmatrix} = P_{to} + P_w + (p_e + p_d)I \quad , \tag{31}$$

and I is a (2 x 2) identity matrix. Utilizing equation (16), in conjunction with equations (26) and (29), then yields

$$P[EI] = \frac{p_d}{n} \sum_{k=0}^{n-1}\sum_{i=0}^{m-1} \binom{n}{k+1}\binom{m}{i+1} p_e^k\, p_d^i \Omega_{k+i} \quad , \tag{32}$$

where

$$\Omega_{k+i} = \frac{1}{2\pi} \frac{(-1)^{k+1}}{k!\ i!} \int_{-\infty}^{\infty}\int_{-\infty}^{\infty} \left(\frac{\omega^2}{2}\right)^{k+1} \exp[j\underline{\omega}'\hat{\underline{X}} - \tfrac{1}{2}\underline{\omega}' P\underline{\omega}]d\underline{\omega} \quad . \tag{33}$$

The remaining task is to determine Ω_{k+1} in terms of the pertinent modeling parameters. This may be accomplished by employing equation (14) and the binomial expansion theorum to explicitly evaluate the integral appearing in equation (33). After integrating and simplifying, equation (33) takes the form

$$\Omega_{k+1} = \frac{\exp\left[\frac{-1}{2}(\hat{\xi}_x^2 + \hat{\xi}_y^2)\right]}{\sqrt{\lambda_x \lambda_y}} \binom{k+1}{k} \sum_{\ell=0}^{k+1} \theta_\ell[\hat{\xi}_x, \lambda_x]\, \theta_{k+1-\ell}[\hat{\xi}_y, \lambda_y] \,, \tag{34}$$

$$\theta_\ell[\xi, \lambda] = \binom{2\ell}{\ell} [-4\lambda]^{-\ell} \sum_{q=0}^{\ell} \binom{\ell}{q} \frac{[-\xi^2]^q}{(2q-1)!!} \,, \tag{35}$$

where $\lambda_{x,y}$ are the eigenvalues of P, given by

$$\lambda_{x,y} = \left[\frac{P(1,1) + P(2,2)}{2}\right] \pm \sqrt{\left[\frac{P(1,1) - P(2,2)}{2}\right]^2 + P^2(1,2)} \tag{36}$$

and

$$\begin{bmatrix} \hat{\xi}_x \\ \hat{\xi}_y \end{bmatrix} = \begin{bmatrix} \frac{\sin\phi}{\sqrt{\lambda_x}} & \frac{\cos\phi}{\sqrt{\lambda_x}} \\ -\frac{\cos\phi}{\sqrt{\lambda_y}} & \frac{\sin\phi}{\sqrt{\lambda_y}} \end{bmatrix} \begin{bmatrix} \hat{X} \\ \hat{Y} \end{bmatrix} \tag{37}$$

with

$$\phi = \tan^{-1}\left[\frac{P(1,1)}{\lambda_x - P(1,1)}\right] . \tag{38}$$

Substituting equation (34) into equation (32), the probability of evader disablement for one attacker is determined as a function of attacker destruction characteristics, attacker trajectory coordinates and associated error statistics, evader localization solution and error statistics, or evader evasion characteristics.

5. MULTIPLE ATTACK PREDICTION

The previous analysis determined the probability of evader disablement for a single attack (equation (32)). In this section, the combined probability of evader disablement is developed when more than one attacker is launched at a single evader. To reduce the complexity of the algorithm, only exponential destruction characteristics (m = 1) are employed, and the termination times for all attackers are assumed to be identical as well as the destruction radii. In addition, trajectory errors are assumed to be zero. From equation (23), the conditional disablement probability distribution for exponential destruct characteristics is given by

$$P[EI|R,1] = \exp[-\xi^2] \ , \tag{39a}$$

$$\xi = R|R_d \ , \tag{39b}$$

$$R = |\underline{X}_{to} + \underline{X}_{ta} - \underline{X}_w| , \tag{39c}$$

where R is the range from attacker to evader at termination.

To determine the probability of evader disablement for multiple attacks, modifications to the problem formulation in the previous sections are necessary. Originally, evader disablement probability was found by integrating equation (5) with respect to R (range from evader to attacker at termination). However, for multiple attackers, there is a termination range for each attacker. To alleviate this problem, trajectory errors are assumed to be zero. Then, equations (6), (7), and (17) reduce to

$$\underline{X} = \underline{X}_t = \underline{X}_{to} + \underline{X}_{ta} \ , \tag{40}$$

$$P(\underline{X}) = \frac{1}{(2\pi)^2} \int_{-\infty}^{\infty}\int_{-\infty}^{\infty} \Phi_X(\underline{\omega}) \exp[j\underline{\omega}'\underline{X}_t] d\underline{\omega} \ , \tag{41}$$

$$\Phi_X(\underline{\omega}) = \Phi_{to}(\underline{\omega})\Phi_{ta}(\underline{\omega}) \ . \tag{42}$$

For multiple attacks, there is a conditional probability distribution for each attacker that takes the form

$$P[EI|R_1] = \exp[-\xi_1^2] \ , \tag{43a}$$

$$P[EI|R_2] = \exp[-\xi_2^2] \ , \tag{43b}$$

$$P[EI|R_N] = \exp[-\xi_N^2] \ , \tag{43c}$$

where $\xi_i = R_i|R_d$ and $R_1, R_2, \ldots, R_N$ are the ranges from the evader to each attacker. If there is no overlap of the destruct regions, the total probability for evader disablement is the sum of the disablement probabilities

from the individual attackers given in equation (32) and can be written as

$$P_T[EI] = P_1[EI] + P_2[EI] + \ldots + P_N[EI] \ . \tag{44}$$

When there is overlap of the regions, which realistically occurs due to the exponential characteristics of the attackers, the individual conditional probabilities must be combined. A formulation well suited to this situation is given by

$$P[EI|R_1, R_2, \ldots, R_N] = 1 - \prod_{i=1}^{N} [1 - \exp(-\xi_i^2)] \ . \tag{45}$$

Substituting equation (43) into (45) and expanding yields

$$\begin{aligned} P[EI|R_1, R_2, \ldots, R_N) = & \sum_{i=1}^{N} \exp[-\xi_i^2] - \sum_{i=1}^{N=1} \sum_{j=1}^{N=i} \exp[-(\xi_i^2 + \xi_{i+j}^2]] \\ & + \sum_{i=1}^{N-2} \sum_{j=1}^{N-i} \sum_{k=1}^{N-i-j} \exp[-(\xi_i^2 + \xi_{i+j}^2 + \xi_{i+j+k}^2)] \ \ldots \\ & + (-1)^{N-1} \exp[-(\xi_1^2 + \xi_2^2 + \ldots + \xi_N^2)] \ . \end{aligned} \tag{46}$$

Recalling that $R = |\underline{X}|$ and employing equations (6) and (24), each exponential for the attack destruction distribution can be written in the form

$$\exp[-(\xi_i^2 + \xi_{i+j}^2 + \ldots)] = \exp\left(-\left[\frac{|\underline{X}_t - \underline{X}_w(i)|^2}{R_d^2} + \frac{|X_t - X_w(i+j)|^2}{R_d^2} + \ldots\right]\right), \tag{47}$$

where

$$\underline{X}_t = \underline{X}_{to} + \underline{X}_{ta},$$

and $\underline{X}_w(\bullet)$ is the position of attacker $(\bullet)$ at termination. Now equation (46) can be written as

$$\begin{aligned} P[EI|\underline{X}_t, \underline{X}_w(1), \underline{X}_w(2), \ldots, \underline{X}_w(N)] = & \sum_{i=1}^{N} \exp\left[-\frac{|\underline{X}_t - \underline{X}_w(i)|^2}{R_d^2}\right] \\ & - \sum_{i=1}^{N-1} \sum_{j=1}^{N-i} \exp\left(-\left[\frac{|\underline{X}_t - \underline{X}_w(i)|^2}{R_d^2} + \frac{|\underline{X}_t - \underline{X}_w(i+j)|^2}{R_d^2}\right]\right) \ldots \\ & \vdots \\ & + (-1)^{N-1} \exp\left(-\left[\frac{|\underline{X}_t - \underline{X}_w(1)|^2}{R_d^2} + \ldots + \frac{|\underline{X}_t - \underline{X}_w(N)|^2}{R_d^2}\right]\right), \end{aligned} \tag{48}$$

and the probability is given by

$$P[EI] = \int_{-\infty}^{\infty}\int_{-\infty}^{\infty} \Phi_X(\underline{\omega})\bar{\Psi}(\underline{\omega})d\underline{\omega} \ , \tag{49}$$

$$\bar{\Psi}(\omega) = \frac{1}{(2\pi)^2} \int_{-\infty}^{\infty}\int_{-\infty}^{\infty} \exp[-j\underline{\omega}'\underline{X}_t] \ P[EI|\underline{X}_t, \underline{X}_w(1), \ldots, \underline{X}_w(N)]d\underline{X}_t \ . \tag{50}$$

As can be seen from equation (48), the first summation weights the destruction capabilities for each attacker individually in the exponential; the double summation averages the destruction capabilities in combinations of two in the exponential; and the triple summation averages the destruction characteristics in combinations of three. This process continues until the last term averages all the destruction characteristics inside the exponential. Equation (48) can be written in the form

$$P[EI|\underline{X}_t, \underline{X}_w(1), \ldots, \underline{X}_w(N)] = \sum_{i=1}^{N} (-1)^{i=1} S_i \ , \tag{51}$$

where S_1 represents the first summation which contains $\binom{N}{1}$ exponential functions, S_2 represents the double summation and has $\binom{N}{2}$ exponential functions, etc. In general for N individual weapons, S_ℓ represents the ℓth summation which has $\binom{N}{\ell}$ exponential functions where $\ell = 1, 2, N$. Substituting equation (51) into (50) results in N integrals of the form

$$\Psi_\ell(\underline{\omega}) = \frac{1}{(2\pi)^2} \int_{-\infty}^{\infty}\int_{-\infty}^{\infty} \exp[-j\underline{\omega}'\underline{X}_t] \ S_\ell d\underline{X}_t \ , \tag{52}$$

where

$$\bar{\Psi}(\underline{\omega}) = \sum_{\ell=1}^{N} (-1)^{N-1} \Psi_\ell(\underline{\omega}) \ . \tag{53}$$

The solution for $\Psi_1(\underline{\omega})$ through $\Psi_N(\underline{\omega})$ is the same except for the number of attackers contained in the exponential. The integral is solved for $\Psi_N(\underline{\omega})$ in the remainder of this section and then the solutions for $\Psi_\ell(\underline{\omega})$ are given. Substituting for S_N in equation (52), $\Psi_N(\underline{\omega})$ is written as

$$\Psi_N(\underline{\omega}) = \frac{1}{(2\pi)^2} \int_{-\infty}^{\infty}\int_{-\infty}^{\infty} \exp[-j\underline{\omega}'\underline{X}_t]$$

$$\cdot \exp\left(-\left[\frac{|\underline{X}_t - \underline{X}_w(1)|^2}{R_d^2} + \ldots + \frac{|\underline{X}_t - \underline{X}_w(N)|^2}{R_d^2}\right]\right)d\underline{X}_t \ . \tag{54}$$

Let

$$\tilde{\underline{\omega}} = \frac{R_d^2}{2}\,\underline{\omega}\,,$$

$$\underline{X}_t = \begin{pmatrix} x \\ y \end{pmatrix},$$

$$\underline{X}_w(i) = \begin{pmatrix} x_i \\ y_i \end{pmatrix},$$

then equation (54) becomes

$$\Psi_N(\underline{\omega}) = \frac{1}{(2\pi)^2} \int_{-\infty}^{\infty}\int_{-\infty}^{\infty} \exp\left(-\frac{N}{R_d^2}x^2 + \frac{2x}{R_d^2}\left[\sum_{i=1}^{N} x_i - j\tilde{\omega}_x\right]\right)$$

$$\cdot \exp\left(-\frac{N}{R_d^2}y^2 + \frac{2y}{R_d^2}\left[\sum_{i=1}^{N} y_i - j\tilde{\omega}_y\right]\right) dxdy$$

$$\cdot \exp\left(-\frac{1}{R_d^2}\left[\sum_{i=1}^{N}(x_i^2 + y_i^2)\right]\right). \qquad (55)$$

From reference 6, the integral becomes

$$\Psi_N(\underline{\omega}) = \frac{R_d^2}{4\pi N} \exp\left[\frac{\tilde{\underline{X}}_N^1\,\tilde{\underline{X}}_N}{NR_d^2} - \frac{1}{R_d^2}\sum_{i=1}^{N}(x_i^2 + y_i^2)\right]$$

$$\cdot \exp\left[\frac{-j\underline{\omega}'\tilde{\underline{X}}_N}{N} - \frac{1}{2}\underline{\omega}'\,\frac{R_d^2}{2N}\,\underline{\omega}\right], \qquad (56)$$

where

$$\tilde{\underline{X}}_N = \begin{pmatrix} \sum_{i=1}^{N} x_i \\ \sum_{i=1}^{N} y_i \end{pmatrix}. \qquad (57)$$

Solutions for $\Psi_1(\omega)$ through $\Psi_{N-1}(\omega)$ can be found in a similar manner. For $\Psi_1(\omega)$, the solution can be reduced to $\binom{N}{1}$ exponential functions of the form

$$\Psi_1(\underline{\omega}) = \frac{R_d^2}{4\pi} \sum_{i=1}^{N} \exp\left[-j\underline{\omega}'\underline{X}_{\omega i} - \frac{1}{2}\underline{\omega}'\frac{R_d^2}{2}\,\underline{\omega}\right] . \tag{58}$$

Similarly, $\Psi_2(\omega)$ has $\binom{N}{2}$ exponential functions and is given by

$$\Psi_2(\underline{\omega}) = \frac{R_d^2}{2(4\pi)} \sum_{i=1}^{N-1} \sum_{j=1}^{N-i} \exp\left(\frac{[\underline{X}_w(i) + \underline{X}_w(i+j)]' \, [\underline{X}_w(i) + \underline{X}_w(i+j)]}{2R_d^2}\right.$$

$$\left. - \frac{x_i^2 + x_{i+j}^2 + y_i^2 + y_{i+j}^2}{R_d^2}\right)$$

$$\cdot \exp\left(- \frac{j\omega'[\underline{X}_w(i) + \underline{X}_w(i+j)]}{2} - \frac{1}{2}\underline{\omega}'\frac{R_d^2}{4}\,\underline{\omega}\right), \tag{59}$$

where

$$\underline{X}_w(\cdot) = \begin{pmatrix} x(\cdot) \\ y(\cdot) \end{pmatrix}. \tag{60}$$

Following this procedure, the remaining solutions for $\Psi_i(\underline{\omega})$ can be found and substituted into equation (53) to obtain $\bar{\Psi}(\underline{\omega})$. Substituting for $\bar{\Psi}(\underline{\omega})$ into equation (49), the probability of evader disablement is given by

$$P[EI] = \sum_{i=1}^{N} (-1)^{i=1} \int_{-\infty}^{\infty} \int_{-\infty}^{\infty} \Phi_X(\underline{\omega})\Psi_i(\underline{\omega})d\underline{\omega} , \tag{61}$$

which can be written as

$$P[EI] = \sum_{i=1}^{N} (-1)^{i-1} P_i[EI] , \tag{62}$$

where

$$P_i[EI] = \int_{-\infty}^{\infty} \int_{-\infty}^{\infty} \Phi_X(\underline{\omega})\Psi_i(\underline{\omega})d\underline{\omega} . \tag{63}$$

Once again, the solution $P_1[EI]$ through $P_N[EI]$ is the same except for the number of weapons contained in the exponential. A solution for $P_N[EI]$ is given, and then the remaining solution can be found. Substituting equations (8), (13), (15), (16), (42), and (56) into equation (63), $P_N[EI]$ can be written in the form

$$P_N[EI] = \frac{R_d^2}{N(2n)} \sum_{k=0}^{n-1} \binom{n}{k+1} \rho_e^k$$

$$\cdot \exp\left[\frac{\tilde{\underline{X}}_N^1 \tilde{\underline{X}}_N}{NR_d^2} - \frac{1}{R_d^2} \sum_{i=1}^{N} (x_i^2 + y_i^2)\, \Omega_{kN}\right] , \tag{64}$$

where

$$\Omega_{kN} = \frac{(-1)^k}{2\pi k!} \int_{-\infty}^{\infty}\int_{-\infty}^{\infty} \left(\frac{\omega^2}{2}\right)^k \exp[j\underline{\omega}'\underline{X}_N - \tfrac{1}{2}\underline{\omega}' P_{XN}\underline{\omega}]\, d\omega \quad , \tag{65}$$

$$\hat{\underline{X}}_N = \hat{\underline{X}}_{to} + \hat{\underline{X}}_{ta} - \frac{\tilde{\underline{X}}_N}{N} , \tag{66}$$

$$P_{XN} = P_{to} + P_e I + \frac{R_d^2}{2N} I . \tag{67}$$

The solution for Ω_{RN} is similar to the solution for Ω_{k+i} (equation (34)) and takes the form

$$\Omega_{kN} = \frac{\exp[-\frac{1}{2}(\hat{\xi}_{XN}^2 + \hat{\xi}_{YN}^2)]}{\sqrt{\lambda_{XN}\lambda_{YN}}} \sum_{\ell=0}^{k} \theta_\ell[\hat{\xi}_{XN}, \lambda_{XN}]\, \theta_{k-\ell}[\hat{\xi}_{YN}, \lambda_{YN}] \tag{68}$$

where $\theta[\cdot,\cdot]$ is given by equation (35), λ_{XN} and λ_{YN} are the eigenvalues of P_{XN} as in equation (36), and the $\underline{\xi}_N = (\xi_{XN}, \xi_{YN})'$ is given by

$$\hat{\underline{\xi}}_N = \begin{bmatrix} \frac{\cos\Phi_N}{\sqrt{\lambda_{XN}}} & \frac{\sin\Phi_N}{\sqrt{\lambda_{YN}}} \\ -\frac{\sin\Phi_N}{\sqrt{\lambda_{YN}}} & \frac{\cos\Phi_N}{\sqrt{\lambda_{YN}}} \end{bmatrix} \begin{bmatrix} \hat{X}_N \\ \hat{Y}_N \end{bmatrix} , \tag{69}$$

$$\Phi_N = \tan^{-1}\left[\frac{P_N(1,2)}{\lambda_{XN} - P_N(1,1)}\right] . \tag{70}$$

Similarly, $P_1[EI]$ can be written in the form

$$P_1[EI] = \frac{R_d^2}{(2n)} \sum_{k=0}^{n-1} \binom{n}{k+1} \rho_e^k\, \Omega_{k1} , \tag{71}$$

$$\Omega_{kl} = \sum_{i=1}^{N} \frac{\exp[-\frac{1}{2}(\hat{\xi}_{Xi}^2 + \hat{\xi}_{Yi}^2)]}{\sqrt{\lambda_{Xi}\,\lambda_{Yi}}} \cdot \sum_{P=0}^{k} \theta_{\ell}[\hat{\xi}_{Xi}, \lambda_{Xi}]\, \theta_{k-\ell}[\hat{\xi}_{Yi}, \lambda_{Yi}] \quad , \tag{72}$$

$$\underline{\hat{X}}_{1i} = \underline{\hat{X}}_{to} + \underline{\hat{X}}_{ta} - \underline{X}_{w}(i), \quad i = 1, 2, \ldots, N \quad , \tag{73}$$

$$P_1 = P_{to} + P_e I + \frac{R_d^2}{2} I \quad , \tag{74}$$

$$\underline{\xi}_{1i} = \begin{bmatrix} \frac{\cos \Phi_1}{\sqrt{\lambda_{X1}}} & \frac{\sin \Phi_1}{\sqrt{\lambda_{Y1}}} \\ \frac{\sin \Phi_1}{\sqrt{\lambda_{Y1}}} & \frac{\cos \Phi_1}{\sqrt{\lambda_{Y1}}} \end{bmatrix} \underline{\hat{X}}_{1i} \quad , \tag{75}$$

$$\Phi_1 = \tan^{-1}\left[\frac{P_1(1,2)}{\lambda_{X1} - P_1(1,1)}\right] \quad , \tag{76}$$

and $\theta[\bullet,\bullet]$ is given by equation (35) and the eigenvalues, λ_{X1} and λ_{Y1}, are given by equation (36). The equations for $P_2(EI)$ ... $P_{N-1}(EI)$ can be formulated in a similar manner and then substituted into equation (62) to obtain the total probability of evader disablement for N attackers.

The previous section has shown that to determine the probability of evader disablement for multiple attackers, the conditional evader disablement probability breaks down to sums of exponentials as is shown in equation (48). For N attackers, each summation averages the destruction characteristics for each attacker individually and in combinations of 2, 3, 4, ..., N. The end result is the total probability of evader disablement is determined by integrating each exponential in all the sums over the entire uncertainty/evasion region ($\underline{X}_{to} + \underline{X}_{ta}$). The attacker trajectory errors can now be included by determining an average trajectory error in each summation. The necessary modifications to the algorithm are presented for the Nth summation in equation (51). Modification to the other summations follow in a similar fashion. For the Nth summation, the average trajectory error can be written as

$$\underline{\bar{X}}_{wN} = \frac{1}{N}(\underline{X}_{w1} + \underline{X}_{w2} + \ldots + \underline{X}_{wN}) \quad , \tag{77}$$

where $\underline{X}_{wi}$ are now Gaussian-distributed random variables. Since the trajectory errors are assumed to be independent Gaussian random variables, $\underline{\bar{X}}_{wN}$ is also Gaussian with the following statistics:

$$E[\underline{\bar{X}}_{wN}] = \underline{\hat{X}}_{wN} = \frac{1}{N} \sum_{i=1}^{N} \underline{\hat{X}}_{wi} \quad , \tag{78a}$$

$$E[(\bar{\underline{X}}_{wN} - \hat{\underline{X}}_{wN})\,(\bar{\underline{X}}_{wN} - \hat{\underline{X}}_{wN})'] = P_{wN} = \frac{1}{N^2}\sum_{i=1}^{N} P_{wi}, \tag{78b}$$

and the characteristic function for $\bar{\underline{X}}_{wN}$ becomes

$$\Phi_{wN}(\underline{\omega}) = \exp[j\underline{\omega}'\hat{\underline{X}}_{wN} - \frac{1}{2}\,\underline{\omega}'P_{wN}\underline{\omega}] \quad . \tag{79}$$

Now equations (40), (41), and (42) can be written in the form

$$\bar{\underline{X}}_N = \underline{X}_t - \underline{X}_{wN} \tag{80}$$

$$P(\bar{\underline{X}}_N) = \frac{1}{(2\pi)^2}\int_{-\infty}^{\infty}\int_{-\infty}^{\infty} \Phi_{\bar{\underline{X}}_N}(\underline{\omega})\exp[-j\underline{\omega}'(\underline{X}_t - \bar{\underline{X}}_{wN})]d\underline{\omega}\ , \tag{81}$$

$$\Phi_{\bar{\underline{X}}_N}(\underline{\omega}) = \Phi_{to}(\underline{\omega})\Phi_{ta}(\underline{\omega})\Phi_{wN}(-\underline{\omega})\ , \tag{82}$$

and equation (54) is now given by

$$\Psi_N(\underline{\omega}) = \frac{1}{(2\pi)^2}\int_{-\infty}^{\infty}\int_{-\infty}^{\infty} \exp[-j\underline{\omega}'(\underline{X}_t - \bar{\underline{X}}_{wN})]$$

$$\cdot \exp\left(-\left[\frac{|\underline{X}_t - \underline{X}_{w1}|^2}{R_d^2} + \frac{|\underline{X}_t - \underline{X}_{w2}|^2}{R_d^2} + \ldots + \frac{|\underline{X}_t - \underline{X}_{wN}|^2}{R_d^2}\right]\right)d\underline{X}_t\ . \tag{83}$$

With the addition of the $\bar{\underline{X}}_{wN}$ term in equation (83), and recognizing that $\tilde{\underline{X}}_N/N = \bar{\underline{X}}_{wN}$, the solution for $\Psi_N(\underline{\omega})$ reduces to

$$\Psi_N(\underline{\omega}) = \frac{R_d^2}{4\pi N}\exp\left[\frac{\tilde{\underline{X}}_N'\,\tilde{\underline{X}}_N}{NR_d^2} - \frac{1}{R_d^2}\sum_{i=1}^{N}(x_i^2 + y_i^2)\right]\cdot \exp[-\frac{1}{2}\,\underline{\omega}'\frac{R_d^2}{2N}\,\underline{\omega}]\ . \tag{84}$$

The next equations that are modified due to the addition of the trajectory errors are equations (66) through (70), which become

$$\hat{\bar{\underline{X}}}_N = \hat{\underline{X}}_{to} + \hat{\underline{X}}_{ta} - \hat{\bar{\underline{X}}}_{wN}\ , \tag{85}$$

$$\bar{P}_{XN} = P_{to} + P_e I + \frac{R_d^2}{2N} I + P_{wN}\ , \tag{86}$$

$$\Omega_{kN} = \frac{\exp[-\frac{1}{2}(\hat{\bar{\xi}}_{XN}^2 + \hat{\bar{\xi}}_{YN}^2)]}{\sqrt{\bar{\lambda}_{XN}\bar{\lambda}_{YN}}}\sum_{\ell=0}^{k}\theta_\ell[\hat{\bar{\xi}}_{XN},\bar{\lambda}_{XN}]\,\theta_{k-\ell}(\hat{\bar{\xi}}_{YN},\bar{\lambda}_{YN}) \tag{87}$$

$$\underline{\xi}_N = \begin{bmatrix} \frac{\cos \bar{\Phi}_N}{\sqrt{\lambda_{XN}}} & \frac{\sin \bar{\Phi}_N}{\sqrt{\lambda_{XN}}} \\ \frac{\sin \bar{\Phi}_N}{\sqrt{\lambda_{YN}}} & \frac{\cos \bar{\Phi}_N}{\sqrt{\lambda_{YN}}} \end{bmatrix} \hat{\underline{X}}_N \quad , \tag{88}$$

$$\bar{\Phi}_N = \tan^{-1}\left[\frac{\bar{P}_{XN}(1,2)}{\bar{\lambda}_{XN} - \bar{P}_{XN}(1,1)}\right] , \tag{89}$$

and λ_{XN}, λ_{YN} are the eigenvalues for P_{XN}.

Following this procedure, the other equations can be modified and the total evader disablement probability can be determined.

6. CONCLUSIONS

This report has presented a real-time computational procedure for predicting the effectiveness of an attacker against a single evader. A functional relationship was developed that expresses the probability of evader disablement in terms of attacker trajectory and associated error statistics, attacker destruction characteristics, and evader localization error statistics and evasion characteristics. Furthermore, the computational algorithm is sufficiently compact to allow for continuous updating of attack performance predictions as tactical conditions change.

Finite-sum Gaussian distributions were used to model the errors associated with estimating evader position after alertment and the attacker destruction characteristics. By selecting the appropriate index (n,m) for each of these finite-sum series, uniform to Gaussian density functions can be obtained to model the pertinent distributions. These two indices are left as inputs to the effectiveness algorithm so as to enhance modeling flexibility and realism.

Finally, the probability of evader disablement was extended to include multiple attacks. To reduce the complexity of the algorithm, only exponential destruction characteristics ($m = 1$) were modeled. In addition, it was assumed that the termination time and destruction radii for all the attackers were the same. The trajectory errors associated with each attacker was also averaged into a single error. Total mission effectiveness was determined by employing the "additive" probability law. An algorithm that predicts total disablement probability for N attackers was subsequently presented.

REFERENCES

1. V.J. Aidala, "Kalman Filter Behavior in Bearings-Only Tracking Applications," IEEE Transactions on Aerospace, Electronic Systems, vol. AES-15, January 1979.

2. E.J. Hilliard, Jr. and R.F. Pinkos, "The Geometry of Escaping Targets," IEEE Transactions on Aerospace, Electronic Systems, vol. AES-14, March 1978.

3. A. Papoulis, Probability, Random Variables, and Stochastic Processes, McGraw-Hill Book Co., New York, 1965.

4. N.N. Lebedev, Special Functions and Their Applications, Prentice-Hall, Inc., New Jersey, 1965.

5. W.B. Davenport and W.L. Root, An Introduction to the Theory of Random Signals and Noise, McGraw-Hill Book Co., New York, 1958.

6. I.S. Gradshteyn and I.M. Ryzhiz, Tables of Integrals Series and Products, Academic Press, New York, 1965.

INITIAL DISTRIBUTION LIST

Addressee	No. of Copies
COMSUBDEVRON 12	1
Assistant Secretary of the Navy (Res, Eng, & Sys)	1
CNO (NOP-098 (2 copies), NOP-22 (2 copies))	4
CNR (OCNR-11 (5 copies), OCNR-12 (5 copies), OCNR-20 (5 copies))	15
SPAWAR (SPAWAR-05)	2
NAVSEA (SEA-06 (2 copies), SEA-63 (4 copies), PMS-409 (2 copies), PMS-416 (2 copies))	10
NOSC (Technical Library)	2
DTIC	2

END

FILMED

MARCH, 1988

DTIC